# Experimental characterization of sub-pixel underwater optical camera communications

Behnaz Majlesein
*LightBee*
Las Palmas de Gran Canaria, Spain
bmajlesein@lightbeecorp.com

Vicente Matus
*IDeTIC-ULPGC*
Las Palmas de Gran Canaria, Spain
vmatus@idetic.eu

Cristo Jurado-Verdu
*IDeTIC-ULPGC*
Las Palmas de Gran Canaria, Spain
cjurado@idetic.eu

Victor Guerra
*Pi Lighting*
Valais, Switzerland
victor.guerra@pi-lighting.com

Jose Rabadan
*IDeTIC-ULPGC*
Las Palmas de Gran Canaria, Spain
jrabadan@idetic.eu

Julio Rufo
*Universidad de La Laguna (ULL)*
San Cristobal de La Laguna, Spain
jrufotor@ull.edu.es

***Abstract*—Underwater Wireless Optical Communication (UWOC) is a promising technology to enable underwater communications for exploring and monitoring marine activities due to its high bandwidth and low latency. Furthermore, underwater optical camera communication (UOCC) takes advantage of light-emitting diodes (LEDs) and cameras already embedded in underwater devices (e.g., drones). In this work, a global shutter-based UOCC system is experimentally tested under a sub-pixel condition, where the dimensions of the LED in the image plane (in µm) are smaller than a single pixel. Although the LED projection dimensions are less than a single pixel, the incoming light irradiance spreads over a limited image sensor area. The results reveal that a 2 m link with a bit rate of 8 bps per channel (24 bps in total) can be attained using an RGB LED as a transmitter and a digital camera as a receiver by applying the point spread function for the demodulation. The validation of this system in sub-pixel conditions guarantees the operation of long-distance UOCC links, where extensive LED sources are perceived as single points in the image. In addition, as the LED dimensions in the image plane are significantly small, the camera can effectively accommodate several transmitters, increasing the link throughput considerably.**

***Index Terms*—Underwater wireless optical communication, underwater wireless sensor networks, optical camera communication, global shutter, point spread function, signal-to-noise ratio.**

## I. Introduction

The demand for ocean exploration is increasing due to the growing need to monitor different phenomena in the underwater environment in many applications, such as oil and gas field exploration, coastal security, environmental impact surveillance, navigation, and ocean-pollution control. Therefore, it is required to establish underwater communication links for the sensor nodes and base stations for signal collection and analysis. Furthermore, remotely operated vehicles (ROVs) and autonomous underwater vehicles (AUVs) are used in such applications, and communicating with them is essential [1]–[3].

This work has been funded by the European Union's Horizon 2020 research and innovation programme under the Marie Skłodowska Curie grant agreement ENLIGHTEM No. 814215
It has also received partial funding from the Spanish State Research Agency, project OCCAM PID2020-114561RB-I00

Cabled or fiber-based approaches can provide a high-speed and reliable communication link. However, those links substantially constrain the link distance and the maneuverability of the underwater nodes. On the other hand, underwater wireless communication systems offer a promising alternative that enables data transmission in unguided underwater environments using wireless carriers. Three leading technologies for underwater wireless transmissions are radiofrequency, acoustic, and optical. Although acoustic systems can establish links over several tens of kilometers, their data rates are considerably low (in the order of kbps), and their latency is high (in the order of seconds) due to the slow speed of the sound in water. Furthermore, they are costly, bulky, and high power demanding [4]. On the other hand, radio frequency (RF) communications are less sensitive to turbulence and temperature gradients. Nonetheless, they are affected by high attenuation in the aquatic environment and the mild Doppler effect. Moreover, they require large size antennas [5]. Alternatively, optical wireless communications technology provides high bandwidth, low latency links, low installation, and operational costs over moderate distances [6]. However, the main limiting factors of underwater wireless optical communication (UWOC) are the absorption and scattering due to the presence of particles in the seawater. These phenomena cause loss of optical intensity and severe temporal pulse broadening, limiting the link distance.

Two main types of light receivers can be used for UWOC: photodetectors (PD) and image sensors [7]. PDs have high reception bandwidth; therefore, they are used mainly in UWOC systems. On the other hand, image sensors provide spatial diversity, which can further increase the number of simultaneous links, and can be found embedded in a wide range of marine devices, such as drones, scuba diver equipment, monitoring camera sensor nodes, etc. Furthermore, the presence of a Bayer filter can enable wavelength multiplexing [8] Therefore, optical camera communication (OCC) technology has increased its popularity in underwater communications, which offers a flexible and low-cost approach for applying in UWOC systems. In [9], [10], a global shutter (GS)-based UOCC was proposed. Their system achieved data rates of 100 bps and 750 bps over a 1 m link range using 12 and 25 LEDs

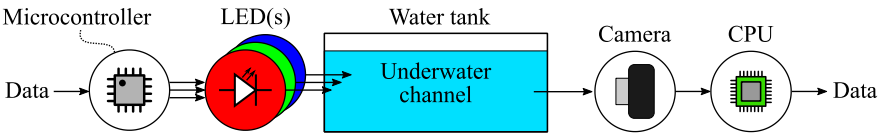

Fig. 1: Block diagram of the proposed GS-based UOCC system.

as transmitters, respectively. The transmitter dimensions were 21 $\times$ 21 cm considering 25 LEDs. The mentioned works had a limited data rate due to the GS mode, restricted by the frame rate. To improve the data rate, a rolling shutter (RS)-based UOCC system was proposed in [11]. In addition, a debbubling algorithm was used to mitigate the bubble distortion on the received images to enhance the communication quality. The authors achieved a data rate of 7.2 kbps in the 1.5 m link range by applying those algorithms simultaneously. However, the RS mode is limited by the source projection size in the image plane, which depends on the link distance, and the physical size of the transmitter to achieve the maximum throughput [12]. In [13], the authors proposed using three different LEDs wavelengths to increase the data throughput by taking advantage of the Bayer filter of the camera, achieving a link throughput of 36 kbps over a 30 cm link range. In [14], three different modulations such as phase-shift keying (PSK), non-return-to-zero on-off keying (NRZ-OOK), and orthogonal frequency division multiplexing (OFDM) in an RS-based UOCC were evaluated and compared under the presence of ambient light. The results demonstrated that PSK was the most robust modulation technique for UOCC under high ambient light conditions.

In the previous works, it is required that the transmitter source projection in the image plane is large enough to establish the link. Otherwise, in GS approaches, sources cannot be detected and spatially differentiated, and, in RS approaches, the throughput is significantly reduced. In conclusion, the link distance is highly limited by the physical size of the transmitter. Increasing the transmitter area will lead to higher deployment costs and power consumption.

Alternatively, in [15] a technique based on the point spread function (PSF) was proposed to increase the SNR in conditions where the dimensions of the light source in the image plane (in µm) are smaller than the area of a single-pixel (i.e., under sub-pixel conditions). This approach benefits from the fact that although the projection size of the LED in the image plane (in µm) is smaller than a single pixel, the incoming light irradiance spreads over a limited area of the image sensor due to the atmospheric scattering, which can be exploited in the demodulation process. Using a 5 mm LED, the authors achieved link ranges of 90 m and 130 m, employing the proposed PSF approach. The mentioned system increases the communication capabilities enabling wireless sensor networks (WSN) in an outdoor environment. Therefore, the design and deployment of underwater sensor networks (UWSNs) [16] can be accomplished by the characterization and evaluation of this approach in an underwater scenario, where the attenuation and scattering phenomena are dominant.

This paper investigates the performance of a GS-based UOCC system over 1 m, and 2 m link ranges using 0.27 $mm$ RGB-LED as a transmitter under a sub-pixel condition. In addition, the system SNR is evaluated and compared for different camera exposure times and analog gains considering two different regions of interest (ROI), including the mask obtained from the PSF and a single-center pixel.

The remainder of this article is organized as follows. First, section II describes the system model, the proposed decoding algorithm, and the evaluation experiments. Then, section III presents and discusses the obtained results. Finally, the conclusion is summarized in section IV.

## II. Methodology

The block diagram of the proposed system model is shown in Fig. 1. This work aims to evaluate the performance of this system under a sub-pixel condition, where the dimensions of the light source projection (in µm) are less than a single pixel. MATLAB R2020b is used to process the received data and measure the SNR. The system performance is evaluated based on the SNR obtained for different camera configurations of the exposure time and the analog gain for two different link distances. Two different ROIs are considered to compare the advantages of using the PSF approach: the ROI detected based on the PSF and a single-center pixel. In the latter case, the selected pixel for the demodulation corresponds to the pixel with the highest value, considered the center of the light source.

### A. Experimental Setup

Figure 3 depicts the experimental setup of the proposed UOCC system. The experiment is carried out in a laboratory environment. The transmitter consists of a 0.27 mm RGB-LED. The LEDs' output power for each color is adjusted to the same peak irradiance using a spectrometer. However, the total output irradiance of each RGB-LED is different depending on the wideness of their spectrum. Figure 2 illustrates the spectral irradiance (W/m$^2$nm) for each RGB-LED channel after the calibration.

At the transmitter side, non-return-to-zero (NRZ) on-off keying (OOK) modulation is used. First, a microcontroller sends data packets with a symbol rate of 7.5 baud, as shown in Fig. 4. Then, each packet is transmitted four times to avoid losing data during the blind time of the camera while processing subsequent frames, guaranteeing that each symbol is captured in at least one frame.

The light propagates through a 1 m water tank filled with tap water. The inner sides of the water tank are covered with a black cover to avoid internal reflections. Note that the transmitter and the receiver are placed outside the water tank. Therefore, the transmitted light traverses four interfaces, namely the air-glass, the glass-water, the water-glass, and the glass-air interfaces, being affected by partial reflections. In

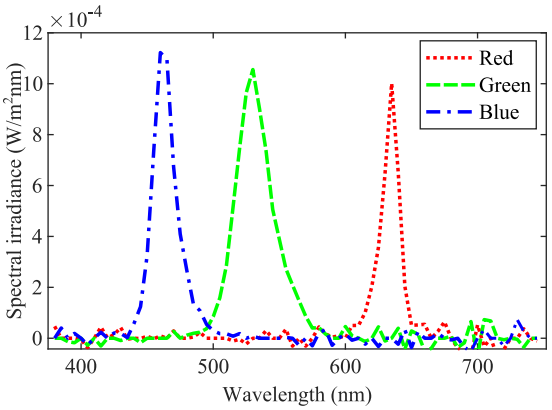


Fig. 2: Emission spectrum of the LED in three different colors.

addition, the glass of the tank is covered with a blue filter film attached to the inner side. This prevents the blue light from leaking out, allowing to perceive the correct color of the marine life inside the aquarium and avoiding the long-term viewing vertigo. This filter impacts the received signal power of the blue channel. Therefore, the air medium experiment is conducted using an empty water tank to avoid a mismatch between the received power for the blue channel in the air and the water medium (due to the presence of a blue filter). On the other hand, to increase the link distance up to 2 m, one mirror is placed at the end of the water tank. The experiments are conducted outside and inside water in 1 m and 2 m link distances, $d$, to compare the attenuation factor of different wavelengths.

A Raspberry Pi Camera Module V2 (based on a Sony IMX219 sensor [17]) configured with a resolution of 1920 $\times$ 1080 pixels, and a frame rate of 30 fps is used on the receiver side. The pixel dimensions are 1.12 $\times$ 1.12 µm. On the other hand, the dimensions of the LED projection in the image plane at 1 m and 2 m are 0.94 $\times$ 0.94 µm and 0.47 $\times$ 0.47 µm, respectively, considering the camera's angle of view (AoV). Therefore, the system works under sub-pixel conditions as the LED projection dimensions are less than the pixel ones.

Highlight that the Bayer pattern of the camera employs two times more pixels for green than red and blue channels. Hence, this channel has more sensitivity than the other two and can effectively affect the system SNR. Therefore, to diminish the effect of the Bayer filter of the camera on the received signal power, two different analog gains for the red and the blue channel to adjust the white balance of the images are considered. In this work, the selected and fixed gains for the red and the blue channels (relative to the green) are $ag_{\mathrm{r}}$= 1.895 and $ag_{\mathrm{b}}$= 1.551, respectively. These values were calibrated experimentally with a white reference source. Moreover, the spectral irradiance of the transmitted power and the spectral responses of the Bayer filter is not perfectly tuned. Consequently, part of the transmitted power for each LED channel is filtered at the camera side. The Raspberry Pi Camera is employed in video capture mode, recording 20 seconds of videos for different exposure times and analog gains, with the digital gain fixed to 1. Those parameters were selected based on the received power for different link ranges to evaluate their impact on the SNR.

TABLE I: Key system parameters.

| Parameter | Value |
|---|---|
| **Transmitter** | |
| LED peak wavelength | Red, Green, Blue |
| LED dimensions (mm) | 0.27 $\times$ 0.27 |
| LED angle of view | 60° |
| Electrical power (mW) | $P_{\mathrm{er}}$ = 0.28, $P_{\mathrm{eg}}$ = 2.73, $P_{\mathrm{eb}}$ = 6.54 |
| Optical irradiance (W/m$^2$) | $P_{\mathrm{or}}$ = 0.017, $P_{\mathrm{og}}$ = 0.036, $P_{\mathrm{ob}}$ = 0.026 |
| Modulation | NRZ-OOK |
| Data rate (bps) | 8 |
| **Channel** | |
| Water type | Tap water |
| Link distance, $d$ (m) | 1, 2 |
| **Receiver** | |
| Camera type | Raspberry Pi Camera Module V2 |
| Image sensor | IMX219 [17] |
| Pixel size (µm) | 1.12 $\times$ 1.12 |
| Camera resolution (px) | 1920 $\times$ 1080 |
| Frame rate (fps) | 30 |
| Exposure time (µs) | 300, 3000, 30000 |
| Analog gain (·) | 1, 5, 10 |
| Focal length, $f$ (mm) | 3.52 |
| Camera angle of view | 38 °(H), 21.4°(V) |
| Optical power meter | Gigahertz-BTS256 |
| White balance gains | $ag_{\mathrm{r}}$ = 1.895 , $ag_{\mathrm{b}}$= 1.551 |

The key system parameters are detailed in Tab. I. The SNR was measured using Gaussian Mixture Model (GMM), using the mask obtained from the PSF and a single-center pixel as the ROIs [15].

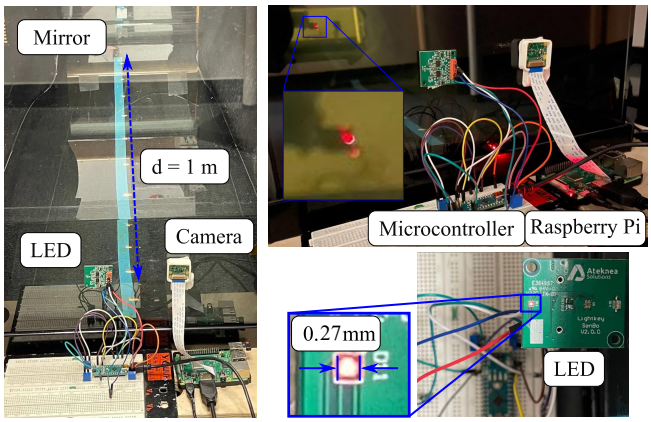


Fig. 3: Experimental setup.

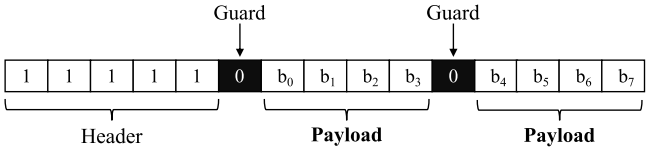


Fig. 4: Schematic diagram of packet structure.

## B. Signal Processing

The demodulation block diagram is illustrated in Fig. 5. First, the videos are captured using the camera module. Then, the frames are extracted from the captured video. Two different ROIs are selected to obtain SNR, including a single-center pixel of the camera and the estimated ROI from the PSF. The

size of the PSF is considered a 5 × 5 px area (around the center pixel), in which pixels have a significantly high cross-correlation. The Gaussian mixture model (GMM), proposed in [18], models the distribution of ones and zeros values using Gaussian distributions and measures the expected value of high or low signal bits and their standard deviation. Then, data is reconstructed using the computed maximum likelihood threshold.

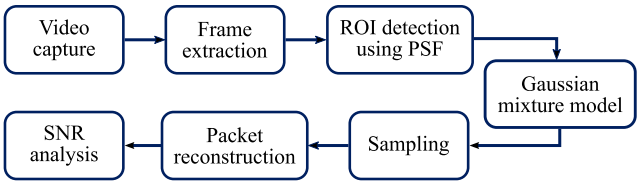


Fig. 5: Decoding process algorithm.

## III. Experimental results

Table II details the measured attenuation factor based on the received signals, which are transmitted through the air and the water medium. The attenuation factors of all the RGB channels are comparable within the 1 m link range. Therefore, for short link distances in UOCC, red LEDs are affected by almost a comparable attenuation factor to blue and green LEDs, making them a good choice for energy-efficient communications [19]. The reason is that the red LED has relatively low power consumption ($P_{er}$) compared to blue ($P_{\mathrm{eb}}$) and green ($P_{\mathrm{eg}}$) LEDs. Moreover, the pixel's photodiode responsivity in the reddish spectral region is higher. However, as the link range increases to 2 m, the attenuation factor for the red wavelength abruptly increases (i.e., 2.2). Figure 6 illustrates images captured for the three LED wavelengths in the air (Fig.6(a)) and in the water (Fig.6(b)) for the 2 m link range and with the camera exposure time ($t_{\mathrm{exp}}$) fixed to 30000 µs and the analog gain (*ag*), to 5. In these images, although the projection size of the LED is less than a single pixel, the light scattered through the medium reaches the neighboring pixels. The number of pixels that receive light coming from the source can be estimated using the correlation in the time domain. It is experimentally measured that this number is roughly the same when the light is transmitted through the air or water. This result is a promising finding because this system can still benefit from the high scattering phenomenon despite the signal being significantly attenuated in water. Furthermore, the light source within the water medium looks more uniformly illuminated in the image compared to the air. Therefore, the scattering in the water medium helps to uniform the received light power, reducing the complexity of the equalization stages. In both environments, the captured illuminated pixels were 10 (H) × 10 (V) for red and green LED colors (based on a fixed normalized threshold pixel value of 0.15). However, despite the LEDs' optical power and the camera's white balance calibration, the blue color values are more attenuated in both images (air and water). This attenuation is due to the blue filter film covering the internal water tank walls. Figure 7 shows an example of the extracted signal for the 2 m link in the conditions mentioned above. The results illustrate that the red channel is the most attenuated compared to the others and the blue channel has the minimum attenuation factor.

TABLE II: Water attenuation factors for RGB channels in 1 m and 2 m link ranges.

| d (m) | R | G | B |
|---|---|---|---|
| 1 | 1.23 | 1.18 | 1.10 |
| 2 | 2.20 | 1.38 | 1.30 |

TABLE III: Comparison between evaluated SNR performance considering two different ROIs in GS-based UOCC experimentally under a sub-pixel condition.

| label | d (m) | ag | $t_{\mathrm{exp}}$ ($\mu$s) | R | G | B |
|---|---|---|---|---|---|---|
| **$\mathrm{SNR_{psf}}$(dB)** | | | | | | |
| (a) | 1 | 10 | 300 | 21.33 | 22.43 | 12.24 |
| (b) | 1 | 1 | 3000 | 22.04 | 19.80 | 12.04 |
| (c) | 2 | 10 | 3000 | 15.70 | 14.80 | 7.25 |
| (d) | 2 | 5 | 30000 | 21.66 | 16.12 | 14.17 |
| **$\mathrm{SNR_n}$(dB)** | | | | | | |
| (e) | 1 | 10 | 300 | 15.50 | 22.04 | Undef. |
| (f) | 1 | 1 | 3000 | 22.02 | 19.79 | 11.96 |
| (g) | 2 | 10 | 3000 | 15.01 | 14.50 | Undef. |
| (h) | 2 | 5 | 30000 | 21.61 | 15.65 | 13.45 |

Table. III shows the comparison of the measured SNR using the PSF approach ($\mathrm{SNR_{psf}}$) and with the single-center pixel receiver ($\mathrm{SNR_n}$) for both 1 m and 2 m link ranges, respectively. According to Tab. III, the SNR was improved significantly with the PSF approach, particularly when the signal is highly attenuated. The SNR for the blue channel using the single-center pixel approach is extremely low in cases (e) and (g), and data cannot be recovered. To account for this, the Tab. III displays the label (*Undef.*). However, the PSF approach can increase the SNR to 12.24 dB and 7.25 dB in cases (a) and (c), respectively.

## IV. Conclusions

In this work, the performance of GS-based UOCC under a sub-pixel condition was assessed. In this condition, the dimensions of the transmitter source in the image plane (in µm) were smaller than a single pixel. The proposed PSF approach could improve the performance of GS-based UOCC systems operating on this condition, enabling UWSNs with higher link distances or smaller transmitter sources that efficiently exploit cameras' spatial multiplexing capabilities. Moreover, as the sources occupy a small area within the images, cameras can be used simultaneously for human and machine-supervised applications, such as underwater video monitoring. The results demonstrated that the proposed GS-based UOCC system model that used a tiny RGB LED source (with dimensions of 0.27 × 0.27 mm) could transmit data with a throughput of 8 bps in 2 m link ranges with SNRs higher than 12 dB thanks to the use of the PSF. Furthermore, due to the small size of the source, several transmitters can be used to increase the throughput effectively. On the other hand, the number of pixels that received energy from the light source due to the scattering was almost the same in both the air and underwater scenarios, regardless of the impact of attenuation of the water. The number of pixels was around 10 (H) × 10 (V) for red and green channels. However, the number of pixels for the blue channel was around 7(H) × 7 (V) because of the

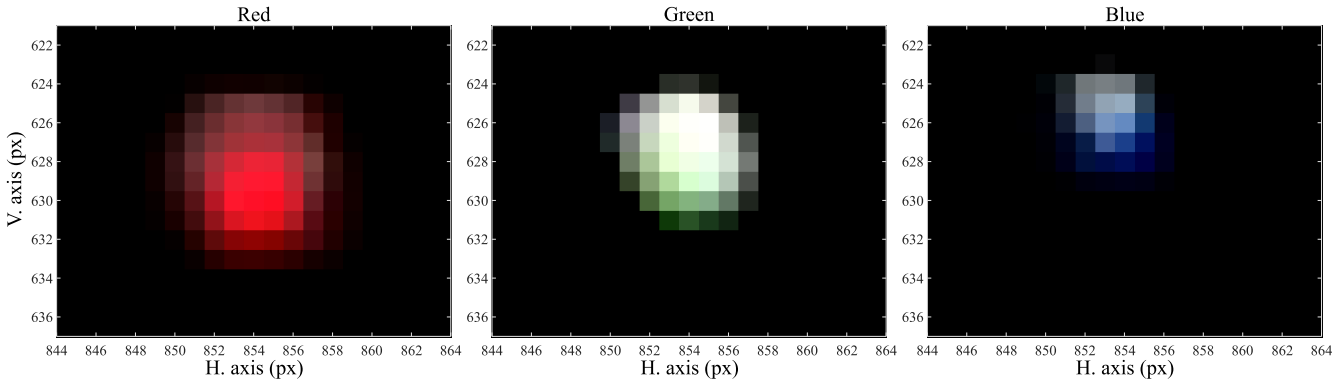


(a) Captured illuminated pixels in air medium.

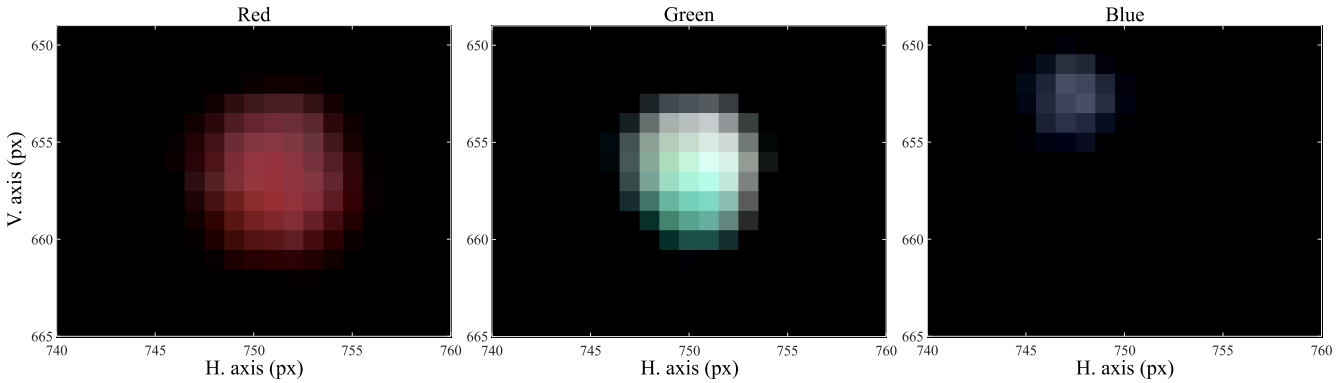


(b) Captured illuminated pixels in underwater medium.

Fig. 6: Captured illuminated pixels in (a) air and (b) underwater medium with $d$ = 2 m, $t_{\text{exp}}$ = 30000 µs, and $ag$ = 5.

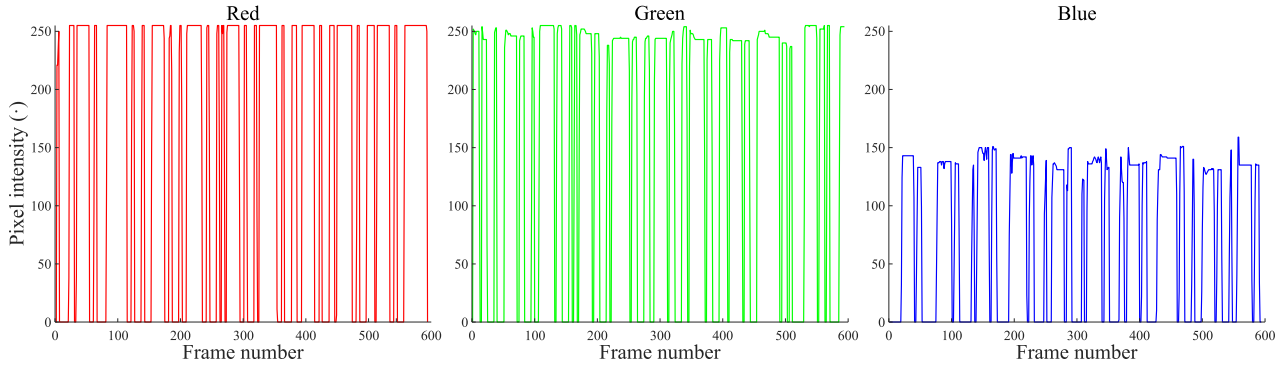


(a) Received signals in air medium.

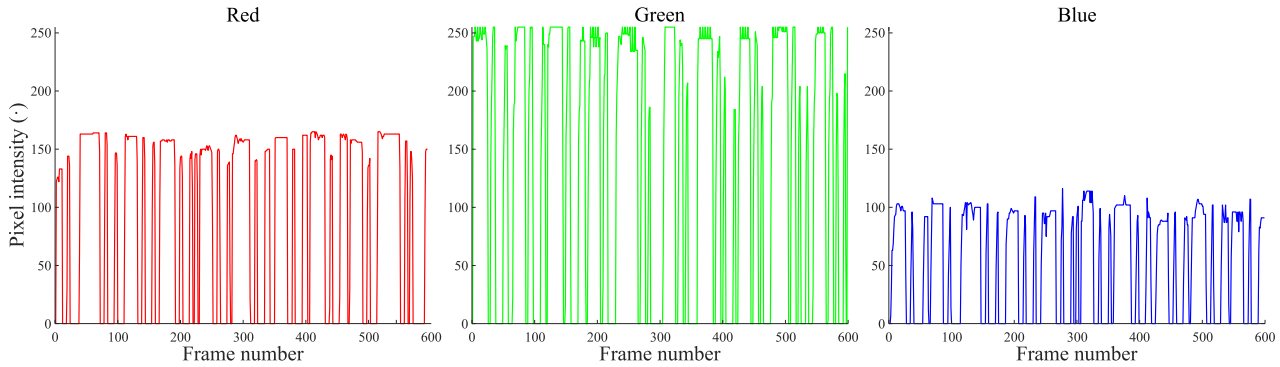


(b) Received signals in underwater medium.

Fig. 7: Received signals in (a) air and (b) underwater medium with $d$ = 2 m, $t_{\text{exp}}$ = 30000 µs, and $ag$ = 5.

blue filter film of the tank glass. Nevertheless, the number of the received pixel area was enough to improve the SNR by using the PSF. The performance and the attenuation factors for the three LED channels were compared for 1 m and 2 m link ranges based on the received signal in the air and the water medium. The results showed that red, green, and blue wavelengths experienced a comparable attenuation within the 1 m link range. However, the red channel was the most attenuated color for the 2 m link range. Therefore, for short link ranges in UOCC, using the red wavelength in the transmitter is a good choice for implementing energy-efficient links. Finally, the results revealed that the PSF approach could significantly improve the SNR, especially when the signal was highly attenuated, as in turbid waters (e.g., coastal and harbor waters).

## REFERENCES


[1] M. Kong, C. H. Kang, O. Alkhazragi, X. Sun, Y. Guo, M. Sait, J. A. Holguin-Lerma, T. K. Ng, and B. S. Ooi, "Survey of energy-autonomous solar cell receivers for satellite–air–ground–ocean optical wireless communication," *Progress in Quantum Electronics*, p. 100300, 2020.

[2] S. Zhu, X. Chen, X. Liu, G. Zhang, and P. Tian, "Recent progress in and perspectives of underwater wireless optical communication," *Progress in Quantum Electronics*, p. 100274, 2020.

[3] X. Sun, C. H. Kang, M. Kong, O. Alkhazragi, Y. Guo, M. Ouhssain, Y. Weng, B. H. Jones, T. K. Ng, and B. S. Ooi, "A review on practical considerations and solutions in underwater wireless optical communication," *Journal of Lightwave Technology*, vol. 38, no. 2, pp. 421–431, 2020.

[4] M. Stojanovic and J. Preisig, "Underwater acoustic communication channels: Propagation models and statistical characterization," *IEEE communications magazine*, vol. 47, no. 1, pp. 84–89, 2009.

[5] A. Palmeiro, M. Martin, I. Crowther, and M. Rhodes, "Underwater radio frequency communications," in *OCEANS 2011 IEEE-Spain*. IEEE, 2011, pp. 1–8.

[6] G. Schirripa Spagnolo, L. Cozzella, and F. Leccese, "Underwater optical wireless communications: Overview," *Sensors*, vol. 20, no. 8, p. 2261, 2020.

[7] M. F. Ali, D. N. K. Jayakody, and Y. Li, "Recent trends in underwater visible light communication (uvlc) systems," *IEEE Access*, 2022.

[8] N. T. Le, M. A. Hossain, and Y. M. Jang, "A survey of design and implementation for optical camera communication," *Signal Processing: Image Communication*, vol. 53, pp. 95–109, 2017.

[9] M. Akram, L. Aravinda, M. Munaweera, G. Godaliyadda, and M. Ekanayake, "Camera based visible light communication system for underwater applications," in *2017 IEEE International Conference on Industrial and Information Systems (ICIIS)*. IEEE, 2017, pp. 1–6.

[10] M. Akram, R. Godaliyadda, and P. Ekanayake, "Design and analysis of an optical camera communication system for underwater applications," *IET Optoelectronics*, vol. 14, no. 1, pp. 10–21, 2019.

[11] Z. Zhou, S. Wen, Y. Li, W. Xu, Z. Chen, and W. Guan, "Performance enhancement scheme for rse-based underwater optical camera communication using de-bubble algorithm and binary fringe correction," *Electronics*, vol. 10, no. 8, p. 950, 2021.

[12] C. Jurado-Verdu, V. Matus, J. Rabadan, V. Guerra, and R. Perez-Jimenez, "Correlation-based receiver for optical camera communications," *Optics express*, vol. 27, no. 14, pp. 19 150–19 155, 2019.

[13] Z. Zhou, S. Wen, and W. Guan, "Rse-based optical camera communication in underwater scenery with bubble degradation," in *Optical Fiber Communication Conference*. Optical Society of America, 2021, pp. M2B–2.

[14] R. Hamagami, T. Ebihara, N. Wakatsuki, and K. Mizutani, "Optimal modulation technique for underwater visible light communication using rolling-shutter sensor," *IEEE Access*, vol. 9, pp. 146 422–146 436, 2021.

[15] V. Matus, V. Guerra, C. Jurado-Verdu, S. Zvanovec, and R. Perez-Jimenez, "Wireless sensor networks using sub-pixel optical camera communications: Advances in experimental channel evaluation," *Sensors*, vol. 21, no. 8, p. 2739, 2021.

[16] S. Arnon, "Underwater optical wireless communication network," *Optical Engineering*, vol. 49, no. 1, p. 015001, 2010.

[17] Sony Corporation, *IMX219PQH5-C, Diagonal 4.60 mm (Type 1/4.0) 8 Mega-Pixel CMOS Image Sensor with Square Pixel for Color Cameras, Datasheet*. Sony Corporation, 2014.

[18] V. Matus, V. Guerra, S. Zvanovec, J. Rabadan, and R. Perez-Jimenez, "Sandstorm effect on experimental optical camera communication," *Appl. Opt.*, vol. 60, no. 1, pp. 75–82, 2021.

[19] V. Guerra Yánez, "Contribution on the study of underwater wireless optical links: channel prediction and energy efficiency," Ph.D. dissertation, Universidad de Las Palmas de Gran Canaria, 2016.